PREPARATION AND CHARACTERIZATION OF Y- AND Bi-BASED BULK AND THIN FILM SUPERCONDUCTORS

by

NITYANAND SINGH

M.SC., I.I.T., Kharagpur, India, 1986

A MASTER'S THESIS

submitted in partial fulfillment of the
requirements for the degree

MASTER OF SCIENCE

Department of Physics

Kansas State University

Manhattan, Kansas

1989

Approved by:

Major Professor

ACKNOWLEDGEMENT

First of all I would like to express my special thanks to my father, mother and brother for their love, encouragement and guidance. I would like to express my sincere thanks to Dr. Michael O'Shea for his valuable advice on this thesis work.

I would like to thank Dr. G. Hadjipanayis and Dr. T. Rahman for serving on my committee.

I thank Dr. G. Hadjipanayis for letting us use his apparatus.

I would like to thank Larry Seib for his assistance and obtaining results using the Electron Microscope.

I would like to thank Dr. B. Depola for letting us use his beam line in J. R. Mcdonald Laboratory.

I would like to thank Prof. Sherwood's group for their assistance in obtaining result using X-ray Photoelectron Spectroscopy.

I would like to thank my Indian friends for their help and friendship.

To the faculty and staff of the Physics Department and my fellow graduate students, I thanks them for their help and encouragement.

CONTENTS

FIGURES

CHAPTER 1

INTRODUCTION

The liquefaction of helium by Kamerlingh Onnes in 1908 led quickly to the discovery of superconductivity in mercury (T_c = 4.2K) in 1911 [1]. In 1913, superconductivity in lead (T_c= 7.2 K) was discovered. The maximum value of T_c for an element is 9.2 K in Nb and was discovered in 1930. Alloys can yield higher values of T_c with the maximum being of 23.2 K for Nb_3Ge. This remained a record until 1986 when Bednorz and Muller detected the appearence of superconductivity in the ceramic La-Ba-Cu-O compounds with a T_c of 40 K [2]. This was soon followed by superconductivity at 90 K in the Y-Ba-Cu-O system in 1987 [3]. Then, a new high T_c superconductor, Bi-Sr-Ca-Cu-O with a T_c of 110 K was discovered [4, 5]. The highest confirmed value of T_c found thus far is in $Tl_2Sr_2Ca_2Cu_3O_8$ with T_c = 125 K [6, 7]. These discoveries have spurred an unprecedented effort by many research groups to explore both the physical mechanism underlying this phenomenon and the obvious technological potential. From both viewpoints, the preparation of the superconducting films is an important step.

The purpose of this work is to prepare bulk superconducting samples of Y-based and Bi- based superconductors and study their properties. I shall also report on some of my efforts to make thin film superconductors.

By now, the preparation of bulk superconduting oxide samples, using solid state reaction, has been well established and reproduced by many groups. On the other hand, preparing thin films of these materials has

turned out to be a more difficult task. Superconducting thin films have been prepared by various processes such as sputtering from bulk material [8], electron beam evaporation [9, 10] and laser ablation of bulk material [11, 12]. Because of the sensitivity of the superconducting transition temperature of the new material to structure and composition, the preparation of thin films has not been easy, generally requiring good control over the processing variables. In this regard, the laser ablation process [11] holds a certain attractiveness because it appears to be relatively insensitive to many of these processing variables. I have therefore chosen the laser ablation process to prepare superconducting thin films.

CHAPTER 2

BRIEF REVIEW

In this chapter we review the general properties of superconductors and the properties of high T_c superconductors.

2.1 General Properties

2.1.1 Type I Superconductors

Bulk superconductors in a weak magnetic field will act as a perfect diamagnet. The flux from an applied field is excluded from the interior of the specimen on cooling the sample through the transition temperature T_c. This is called the Meissner effect. The simple result

$$B = H + 4\pi M = 0$$

follows from this for temperatures $T < T_c$. This leads to a diamagnetic suceptibility

$$\chi = M/H = -1/4\pi$$

When the difference in free energies of the normal and superconducting states are equal to the volume magnetic field energy, the magnetic flux will penetrate and the sample will become normal. The applied field B_c at which this occurs is known as the critical field and is usually written in terms of H_c (units are numerically the same in cgs). Such superconductors are known as type I superconductors. Magnetization versus applied magnetic field for a type I superconductor is sketched in figure 2.1 (a)

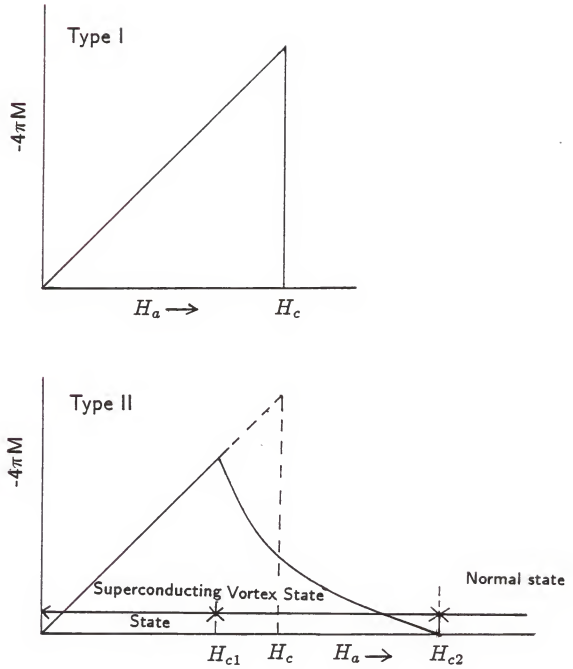

Fig. 2.1 Magnetization vs. applied magnetic field for (a) type I

(b) type II bulk superconductor.

2.1.2 Type II Superconductors

In type II superconductors the magnetic flux penetrates at some lower critical field H_{c1} and fully penetrates destroying the superconductivity at some upper critical field H_{c2}. For $H_{c1} < H < H_{c2}$ the superconductor is in a mixed states where bulk superconductivity is still present but magnetic flux penetration in the form of tubes (magnetic vortices) has occured. This phase diagram is illustrated in figure 2.1 (b). All high T_c superconductors are of this type. These magnetic vortices may become pinned leading to hysteresis in the M - H curves as illustrated in figure 2.2 (a) (no hysteresis) and figure 2.2 (b) (hysteresis present).

2.1.3 Critical Current Density J_c

For type I superconductors a simple relationship exists between J_c and H_c. Since no magnetic flux penetrates into the interior of the sample, all the current flows on the surface. In fact a small penetration of B into the material does occur (London penetration) and the superconductor current flows in the near surface region. The current that produces a magnetic field of H_c at the surface of the sample is the critical current.

For type II Superconductors, the magnetic vortices can be pinned and there is no simple relation between the critical field and J_c. In order for the superconductor to transform into the normal state the magnetic vortices must be unpinned to allow the field to penetrate. A phenomenological model due to Bean, the so-called critical state model [13], gives a relationship between the remanent magnetization M_r and the critical current density J_c

$$J_c = 15\ M_r\ /\ \mathrm{R}$$

for a cylindrical sample of radius R in cm with the applied field along the cylinder axis. M_r is in emu/cc.

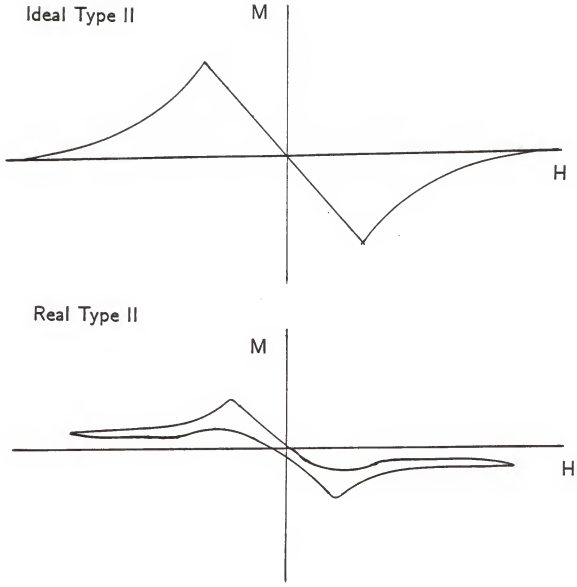

Fig 2.2 (a) Hysteresis curve for ideal type II superconductor.

(b) Hysteresis curve for type II superconductor with flux pinning.

2.2 High T_c Superconductor

A number of families of high T_c superconductors have now been discovered. These include the La-Ba-Cu-O system with a tetragonal structure which have T_c's as high as 40 K [2], the $RBa_2Cu_3O_{7-y}$ (R=Y,Gd,Ho,Er) with T_c's as high as 93 K [3] which have an orthorhombic structure and the A-Ca-Sr-Cu-O systems where T_c's range from 110 K (A = Bi) [4, 5] to 125 K (A = Tl) [6, 7]. All of the above families contains Cu - O planes and it is believed that this Cu - O structure is responsible for superconductivity.

2.3 Thin Films

A number of thin film superconductors have now been prepared by a variety of methods including laser ablation [11, 12], evaporation [9, 10], annealing of multilayers [14], sputtering [8] and molecular beam epitaxy [15]. In nearly all cases a high temperature anneal was required of the deposited material, even in cases where the target from which the material was deposited had been demonstrated to be superconducting. We will discuss some cases below where an anneal is not required.

The substrate used in deposition has a strong influence on the microstructure and superconducting properties of the deposited film. $YBa_2Cu_3O_{7-y}$ films deposited on $SiTiO_3$, Al_2O_3, MnO and ZrO_2 are superconducting with films on $SiTiO_3$ (100 face) generally having the best superconducting properties (highest T_c, sharpest transition, largest J_c). The reason for this is that the 3.40 A (cubic) lattice constant is close to that of the [100] face of $YBa_2Cu_3O_{7-y}$ resulting in very little strain in the film. Critical currents of 10^6 amps/cm^2 have been reported at 4.2 K in such films.

For similar reason Bi - Ca - Sr - Cu - O films deposited on MnO (100 face) have the best superconducting properties.

In order for superconductors to achieve widespread technological usefulness two problems must be overcome.

(i) Deposition of superconductors on Si and SiO_2

In order for high T_c superconductors to be used with Si technology a method must be developed to deposit films which are superconducting directly on Si or SiO_2.Thus far no oxide film has been deposited directly on Si or SiO_2 and found to be superconducting after a high temperatures anneal although a numbers of attempts have been reported [16, 17]. Buffer layers of metals such as Au in between the substrate and film do allow superconducting films to be grown .

(ii) High Temperature Anneal

It is necessary in almost all preparation methods to anneal the superconductor at high temperature (700^oC) in an oxygen rich environment in order to crystallize the right structure and incorporate enough oxygen into the film to make it superconducting. Since the substrate is also annealed at the high temperature, annealing may (a) modify the properties of the substrate (any doped semiconductor in contact with the superconductor will have its properties modified with, for example, a phase separation of dopants) and (b) produce interdifussion between the substrate and film. This latter effect has been shown to destroy the superconducting properties of very thin $YBa_2Cu_3O_{7-y}$ films on $SiTiO_3$. In order for these problems to be avoided the high temperature anneal must either be bypassed or the annealing temperature must be substantially lowered.

Laser ablation shows promise in elleviating both problem (i) and (ii). In

the laser ablation process chunks of superconducting materials are deposited on the Si or SiO_2 substrate. Expitaxial growth does not occur on the substrate and a fine-grained film is usually obtained. It is hope that the material will however retain its structure and oxygen content, so that an anneal to epitaxially regrow the film and incorporate oxygen will not be required.

CHAPTER 3

SAMPLE PREPARATION AND EXPERIMENTAL APPARATUS

3.1 Preparation of Bulk Superconductor

All bulk superconductor samples are synthesized by the solid state reaction using the appropriate amount of oxide of each element and are mixed after grinding. The oxides used were (1) Y_2O_3, $BaCO_3$ and CuO for Y-Ba-Cu-O superconductors and (2) Bi_2O_3, CuO, $SrCO_3$ and CaO for Bi-Sr-Ca-O superconductors. These powdered oxides were then pressed into pellet form at 10,000 PSI with a die and hydraulic press. The pellets were 1 centimeter square and few millimeter thick. The Pellet was removed very carefully because it was fragile and was placed on a crucible in a furnace and heated (sintered) at the appropriate temperature (Y-based 950 $\pm 25^{o}C$ and Bi-based 750 $\pm 25^{o}C$ for 8 hours. Then the furnace was turned off and the sample was slowly cooled to below $200^{o}C$ in 4 hours. This process was repeated once. The final product is a somewhat porous square sample. If it was superconducting it was black in color and if not it was usually a dark grey.

3.2 Preparation of Superconductor Thin Films

Thin films of the high temperature superconductor perovskite $YBa_2Cu_3O_{7-y}$ and Bi-Sr-Ca-Cu-O systems were deposited on silicon and carbon fiber substrates by laser ablation of the bulk material. A schematic diagram of the aparatus for this technique is shown in figure 3.1. The radiation from a pulse excimer laser operating at 193 nm is focused onto

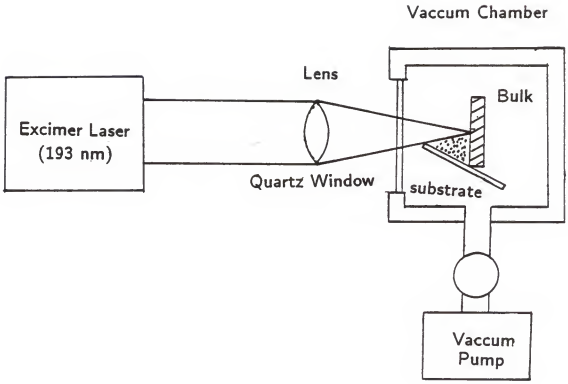

Fig. 3.1 Schematic diagram of set up used for making thin films.

a target which is bulk sample of the material to be deposited. The substrate surface is oriented at approximately 45° to the bulk sample, with a target to substrate distance of 5-10 mm. Both the target and substrate are contained in a vacuum cell. The laser was operated at repetition rates between 5 and 20 pps (pulses per second) with an energy of 90 mJ per pulse focused to approximately 0.5 mm^2 at the sample. The target was rotated slowly in order to remove material uniformly from the bulk sample. The deposited film obtained by this method was non-uniform in thickness with the maximum thickness in the range of few thousand angstroms.

3.3 Structure and Composition Characterization

3.3.1 X-ray Diffraction

To determine the structure of the superconductor x-ray diffraction measurements were performed using a Philips x-ray diffractometer located in Agronomy. Cu-K raditation is used as the x-ray source. Diffracted signals are detected by a proportional counter. Then using Bragg's law, we can find spacing (d) between atomic planes

$$2\text{d } \sin\theta = n\lambda$$

where θ is incidence angle and λ is the wavelength. Again we know that for an orthorhombic structure

$$1/d^2 = h^2/a^2 + k^2/b^2 + l^2/c^2$$

Where a,b,c are primitive vectors of the crystal lattice and h,k,l are integers. So by calculating d values we can find the separation of the different planes present in the superconductor which we may then use to identify the structure of the superconductor.

3.3.2 Energy Dispersive X-ray (EDX) spectrometers

Energy dispersive X-ray (EDX) analysis was done within an electron microscope using a SiLi detector. X-rays enter through the thin beryllium window and produce electron-hole pairs in the SiLi. The energy of each incident photon can be measured and the output presented as an intensity versus energy display. The main advantage of EDX detectors over a diffractometer is that simultanous collection of the whole range of X-rays is possible and an indication of all the elements (with atomic number greater than sodium) can be obtained in a matter of minutes. But it is not surface sensitive since the xray signal may emerge from deep within a bulk sample or film. If a film is very thin (less than 5000 A) a strong xray signal from the substrate may be obtained.

3.3.3 Rutherford Backscattering (RBS)

The RBS setup is shown in figure 3.2. Li^{2+} ions (3 MeV energy) produced by the Tandem Van de Graff located in the Macdonald atomic physics laboratory, were used as a projectile. By observing the energy spectrum of the scattered ions, a profile of the various elements in the sample (but only elements with m_2 (target mass)$> m_1$ (projectile mass)) may be obtained. First we consider elastic scattering of the projectile energy E_o and mass M_1 from the surface . From conservation of energy and momentum the final energy E_1 of the projectile after scattering through some angle θ is given by

$$E_1 = E_0((M_2^2 - M_1^2 sin^2\theta)^{1/2}/(M_2 + M_1))^2$$

The energy ratio K=E_1/E_0, called the kinematic factor, is determined only by the masses of the incident ion, target ion and the scattering angle.

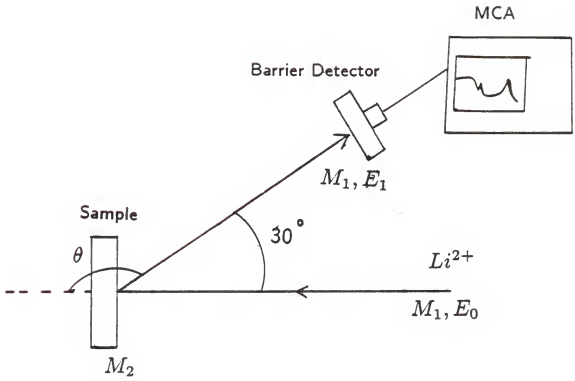

Fig. 3.2 Schematic of Rutherford backscattering set up.

Different elements in the material yield different kinematic factors and thus using RBS we can determine the elements present at the surface of the superconductor. This is indicated schematically in figure 3.3 (a) for $YBa_2Cu_3O_7$. If the projectile ion penetrates the surface and scatters from an atom in the bulk it will lose energy during the time it spends in the solid. The signal from the ion is shifted to lower energies for these ions and this is indicated schematically in figure 3.3 (b). Adding up the signals from Y, Ba, Cu, O gives spectrum of figure 3.3 (c), the final RBS spectrum.

3.3.4 X-Ray Photoelectron Spectroscopy (XPS)

The basic processes of interest in photoelectron spectroscopy are the absorption of a quantum of energy $h\omega$ and the ejection of an electron, the photoelectron, whose kinetic energy, referenced to an appropriate zero of energy, is related to the binding energy of an electron in the target atom. In this process, an incident photon transfers its entire energy to the bound electron. The core level energies of the elements are well known and are only influenced weakly by chemical bonding and the state of the ion in the solid. The small shift in the binding energy of core levels can be messured and may be used to determine chemical information on the state of the ion as we discussed in section 4.1.3. Element identification is provided by the binding energy of the electrons that escape from the surface using

$$E_B = E_{KE} - h\omega$$

Since the escape depth of the electron is of order 20 A in the keV range, this measurment is surface sensitive and thus useful for very thin films.

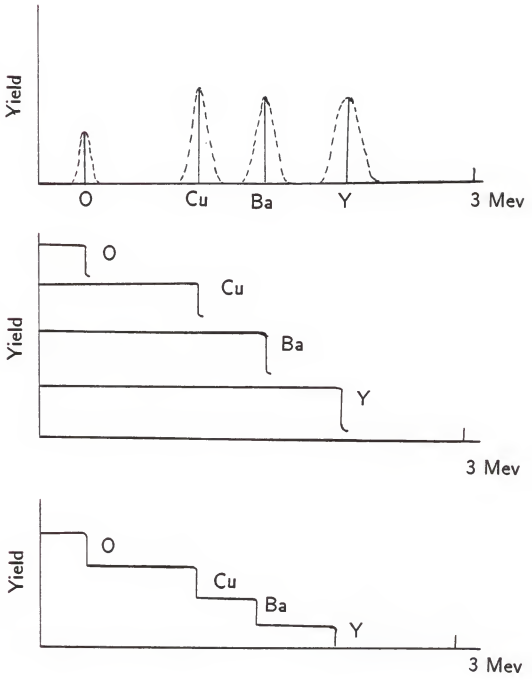

Fig. 3.3 (a) Schematic RBS signal from surface only for $YBa_2Cu_3O_7$.

(b) Schematic RBS signal inside the sample for $YBa_2Cu_3O_7$.

(c) Schematic RBS spectra for (a) and (b) combined together.

3.4 Magnetic and transport measurements

3.4.1 AC Susceptibility

AC Susceptibility measurements are made using the apparatus shown schematically in figure 3.4. There are two sets of coils which are wound onto a delrin coil former and placed at the end of a probe. One is a modulation coil which provides an ac field $H_a = H_{0a}cos(\omega t)$. The other is a set of pick-up coils which are wound in series opposition and are inside the modulation coils. Without a sample, the signal induced in the upper and lower halfs of the pick-up coils cancels out. With a sample inside the lower half of the pick-up coils the emfs become unbalanced and a signal proportional to the ac susceptibility (after lock-in detection) is obtained. Temperature is measured using a calibrated Si diode and temperature is varied by lowering the ac susceptibility probe slowly into a helium dewer. The temperature accuracy is estimated to be $\pm$ 1.5%.

3.4.2 Superconducting Quantum Interferometer Device (SQUID)

A Josephson junction loop is used to measure the magnetic flux of a sample and after calibration (by the manufacturer) yields the magnetic moment. This is done by mechanically moving the sample through the superconducting loop. The temperature and magnetic field are controlled by computer and a long sequence of data taking may be programmed. Temperature is controlled to within 0.2% when a measurement is taken.

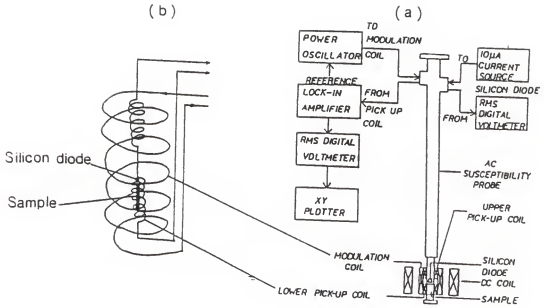

Fig. 3.4 (a) Schematic of ac susceptibility apparatus.

(b) The two sets of coils in ac susceptibility probe.

3.4.3 Resistivity Measurment

Resistivity measurment were performed using a four probe system. Here we pass a fixed current through a superconductor using two current leads which sandwitch two voltage leads. This arrangement would avoid the voltage drop to the sample by the current connecting wire. This measurment is done inside the He dewar and the temperature of the sample is changed by raising and lowering the resistivity probe. The temperature is measured using a silicon diode placed close to the sample and the temperature accuracy is estimated to be $\pm$ 1.5%.

CHAPTER 4

BULK SUPERCONDUCTORS

4.1 Structure and Composition of Superconducting Compounds

In this chapter we discuss our studies on bulk Y-based and Bi-based superconductors. The following measurment were made to confirm structure and composition of the sample:

4.1.1 X-Ray

A number of samples were xrayed to check their structure. Figure 4.1 (b) shows the X-ray diffractogram for a $YBa_2Cu_3O_{7-y}$ superconductor. It was found that all the peaks could be associated with the $YBa_2Cu_3O_{7-y}$ orthorhombic structure. The best values of a, b and c are 3.82 Å, 3.89 Å and 11.67 Å. Figure 4.1 (a) shows the X-ray diffractogram for a Bi-based superconducting sample and it was found that all the peaks could be associated with the $Bi_2Sr_1Ca_2Cu_2O_{8-y}$ structure (2122 phase) indicating that the material is polycrystalline single phase 2122 material. The best values of a and c are 5.41 Å and 30.85 Å.

4.1.2 Electron Microscopy

The morphology of the superconductor was examined by electron microscopy. Figure 4.2 shows a blow-up of the individual grains after sintering. It can be seen that a small amount of melting has occured in addition to the solid state reaction. The size of the grains are 1μm.

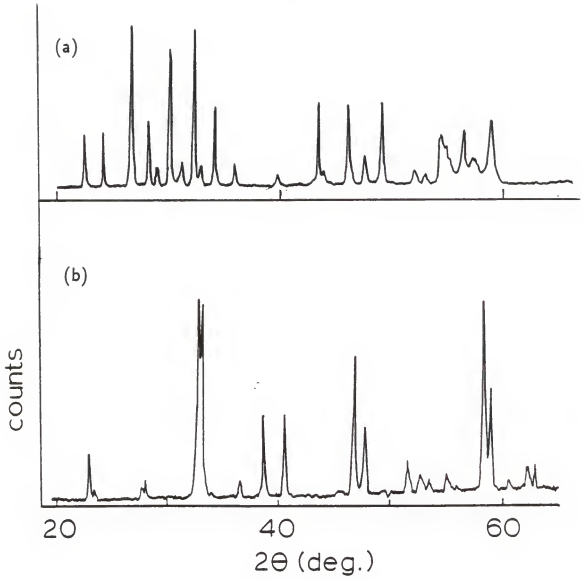

Fig. 4.1 X-ray diffractogram of

(a) $Bi_2Ca_1Sr_2Cu_2O_{8-y}$ bulk superconductor.

(b) $YBa_2Cu_3O_{8-y}$ bulk superconductor.

Fig 4.2 Electron microscope photograph of $YBa_2Cu_3O_{7-y}$ surface

1000 X magnification.

4.1.3 X-ray Photoelectron Spectroscopy (XPS)

XPS measurements were made using a VSW HA 100 spectrometer with a base pressure of 10^{-10} TORR using Mg K X-radiation by Prof. Sherwoods group. We will report only the results here. XPS study showed the presence of all the 5 elements, Bi, Sr, Ca, Cu and O in a scintered $Bi_2SrCa_2Cu_2O_{8-y}$ sample. Small shifts of the core levels can be used to infer the oxidation state of the ion. The elements, Bi, Ca, Sr and O are in their usual formal oxidation states of +3, +2, +2 and -2 respectively. Cu is more difficult to interpret but XPS results indicate significant amounts of Cu^{1+} and Cu^{2+}. Assuming that the bonds are ionic and y=0 (no crystals is completely ionic in reality), we find that Cu has a +2 formal oxidation state. In reality the charge on the Cu will be some what less than the above number since the bond will be partially covalent. The situation in $YBa_2Cu_3O_{7-y}$ is more complex. In $YBa_2Cu_3O_{7-y}$, the valence states from XPS are found to be +3, +2 for Y and Ba respectively. There are two type of Cu site in the crystal and balancing charge and assuming a completely ionic crystal indicate that both $Cu^{2+}$and Cu^{3+} are present for y=0.

4.2 Y-Based Superconductors

A number of $YBa_2Cu_3O_{7-y}$ compounds were made and it was found that a low annealing temperature (700° C) led to non-superconducting compounds down at 4.2 K. A sample annealed at 950° C was chosen for some detailed measurments. The resistivity measurment was performed and it shows zero resistance around 93 K as shown in figure 4.3.

The ac suceptibility was measured using the apparatus shown in fig.(3.3). The measurment was performed by slowly cooling the sample from

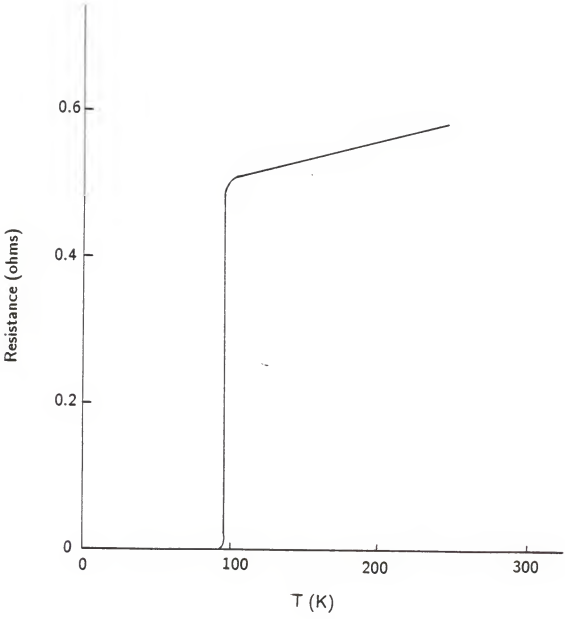

Fig. 4.3 Resistance vs. Temperature plot for $YBa_2Cu_3O_{7-y}$ bulk superconductor.

well above T_c, and a diamagnetic response was observed at 93 K as shown in figure 4.4 (a).

The magnetization versus temperature curve obtained from the SQUID magnetometer is shown in figure 4.5 and there is a large diamagnetic response around 93 K. In the superconducting state

$$B = 4\pi M + H = 0$$

so that the expected suscptibility for the superconductor for $H < H_{c1}$ is

$$\chi = M/H = -1/4\pi$$

By compairing M/H with - $1/4\pi$ at 4.5 K we found that approximately 80 % of the sample is superconducting.

Figure 4.6 shows a hysteresis loop taken in the SQUID magnetometer at 10 K. As can be seen, strong hysteresis is present due to flux pinning. The zero field (remanent) moment yields a critical current of $7.6X10^3$ amp/cm^2, according to the critical state model. H_{c1} was determined from the magnetization curves shown in figure from the point where the intial curve departs from linearity. At 10 K H_{c1} is 2.0 $\pm$ 0.1 kOe.

4.2.1 Effects of Element Substitution

We find substitution of Gd or Er for Y only produced a small effect on T_c. Xrays show that these sample have the same structure as $YBa_2Cu_3O_{7-y}$. In the case of Co, substitution for Cu decreases T_c drastically. For 4 % substitution of Cu by Co decreases T_c to 55K and for 8 % substitution of Co, the sample was not a superconductor. These results suggest that the rare earth site is not important in determining superconductor properties but the Cu-O structure is.

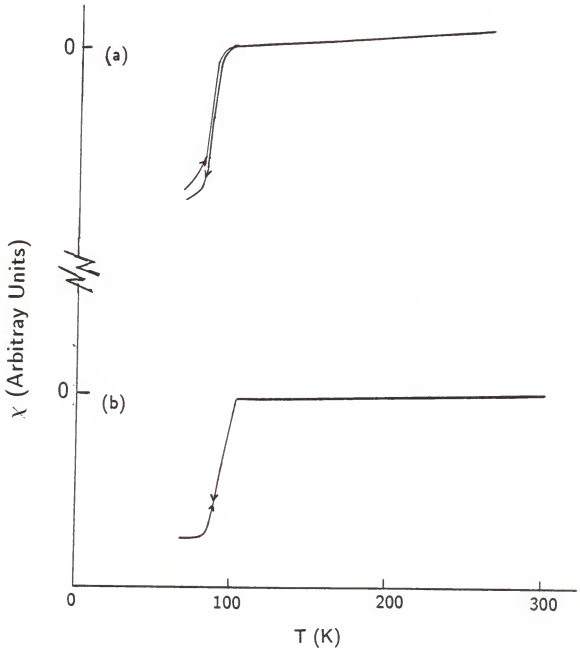

Fig.4.4 ac susceptibility curves for

(a) $YBa_2Cu_3O_{7-y}$ bulk superconductor.

(b) $Bi_2Ca_1Sr_2Cu_2O_{8-y}$ bulk superconductor.

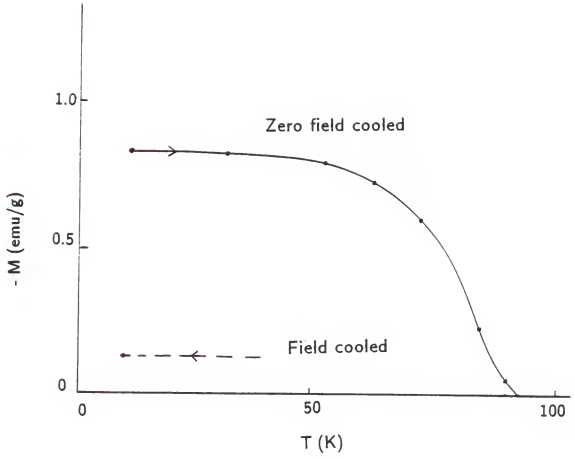

Fig. 4.5 M vs. T plot for $YBa_2Cu_3O_{7-y}$ bulk superconductor.

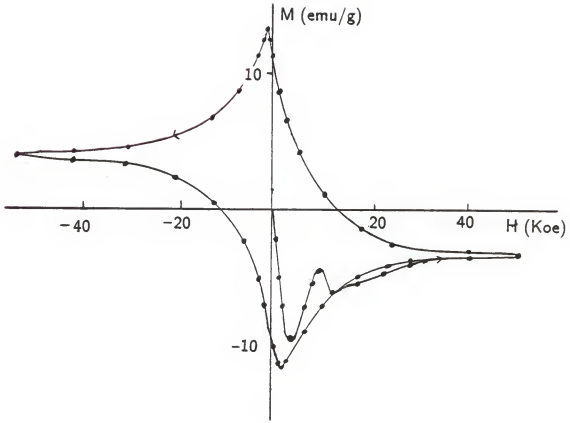

Fig. 4.6 Hysteresis loop for $YBa_2Cu_3O_{7-y}$ at 10 K taken in SQUID.

4.3 Bi-Based Superconductors

SQUID magnetometry and ac susceptibility were used to test for superconductivity. The ac susceptibility measurments showed a transition to a superconducting state at about 80 K. SQUID magnetometer measurments revealed an additional transition at 105 K. The magnetisation versus temperature curves (both zero field and field cooled) obtained from the SQUID are shown in figure 4.7 and there is a small diamagnetic response at 105 K followed by a much larger diamagnetic response at about 80 K. A comparision of M/H (after zero-field-cooling the sample) with 1/4 indicates that approximately 0.2 % of the sample is superconducting below 110 K and 60 % of the sample is superconducting below 80 K. The 80 K transition is associated with the 2122 phase which was the only phase detected in xrays and it is likely that the 110 K transition is associated with a small amount of 2223 phase, undetected in xrays. As with other high T_c superconductors the field-cooled value of M is considerably reduced from its zero-field-cooled value.

Figure 4.8 shows a hystersis loop taken in a SQUID magnetometer at 4.5 K. As can be seen, strong hysteresis is present. The zero field (remanent) moment yields a critical current of $3.0X10^3$ Amp/cm^2 according to the critical state model. Initial magnetization curves are shown in figure 4.9 at 4.2 K, 40 K and 77 K. At 4.5 K H_{c1} is 1.5 kOe and falls to 200 Oe at 40 K and approximately 20 Oe at 77 K. As shown in the insert to figure 4.8 the remanent moment decreases with time as found with other superconductors. The dependence on time is approximately logaritlmic.

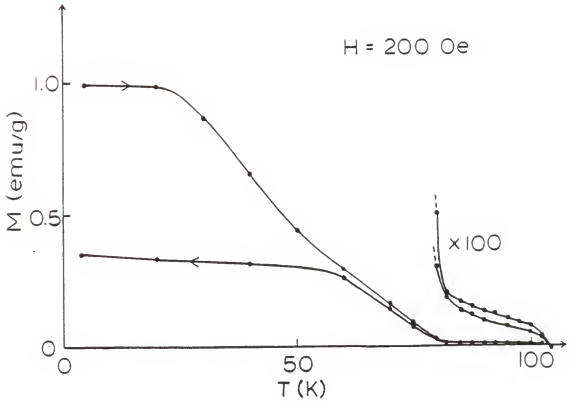

Fig. 4.7 M vs. T plot for $Bi_2Ca_1Sr_2Cu_2O_{8-y}$ bulk superconductor.

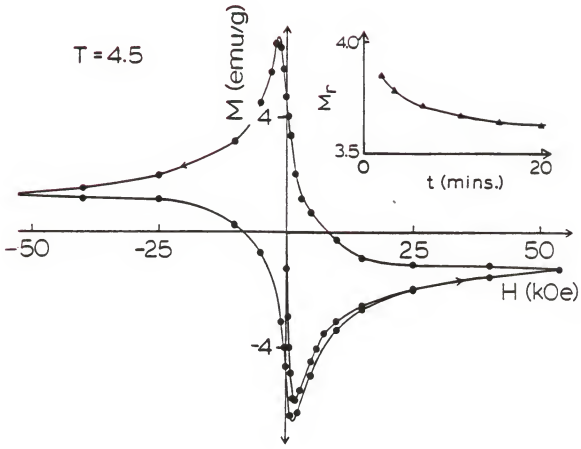

Fig 4.8 Hysteresis loop for $Bi_2Ca_1Sr_2Cu_2O_{8-y}$ at 4.5 K and remanent variation with time.

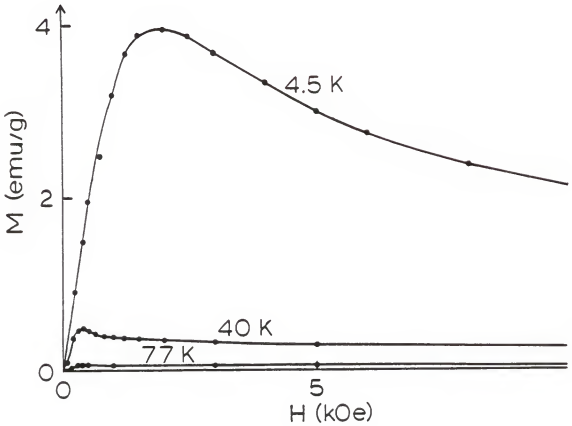

Fig. 4.9 Initial magnetization curve for $Bi_2Ca_1Sr_2Cu_2O_{8-y}$ at different temperature.

CHAPTER 5

THIN FILMS

5.1 Introduction

Thin films were prepared by laser abalation of superconductor bulk materials. A vacuum was required to prepare the thin films. The goal of this part of the work is restricted to determining the structure and composition of the films. Thickness of the deposited film can depend on the sample geometry, the pulse energy density, the number of pulses incident on the superconductor and the vacuum conditions in the chamber. The thin films were prepared on Silicon and Carbon fibre substrates. These films were deposited at room temperatures. Evaporation of the sintered material under vaccum ($\approx 10^{-7}$ Torr) in the case of Bi - Sr - Ca - Cu - O compounds produced films of almost pure Bi. This method of thin film preparation was not pursued any further.

5.2 Structure, Composition and Properties of Thin Films on Si

$YBa_2Cu_3O_{7-y}$ and $Bi_2Sr_1Ca_2Cu_2O_{8-y}$ superconductors were deposited on Si and carbon fiber substrates by laser ablation. The initial films, however, were not thick but subsequently I was able to prepare thicker films by increasing the pulse rate of the Excimer laser and improving the vacuum ($\approx 10^{-4}$Torr) in the chamber.

5.2.1 Rutherford Back Scattering (RBS)

The RBS measurements were performed in the Macdonald laboratory

using Li^{2+} ions. Measurements were performed on both thin film and bulk sample. Figure 5.1 (a) shows the RBS spectrum of bulk $YBa_2Cu_3O_{7-y}$ sample and the edges for the Y, Ba and Cu are easily discernable. The arrows mark the expected position of the edge according to equation 3.1. The oxygen edge is not discernable in the spectrum. Figure 5.1 (b) and (c) show spectra for films approximately 500 Å and 1000 Å thick respectively. Again all the elements except oxygen have edges which are easily discernable. A large signal from the Si substrate is also present in the case of thin films.

In the case of the Bi-based superconductor films a Bi edge was discernable as shown in figure 5.2 but no clearly discernable edges are present for the other elements, only a broad increasing background.

5.2.2 Energy Dispersive X-ray Analysis (EDX)

EDX measurments were performed using the Transmission Electron Microscope. In the case of the bulk material all elements (except O,which is not detectable using the preset set-up, were detected) as can be seen from figure 5.3 (a) and figure 5.4 (a). In thin film form we were not able to clearly discern Y and O in the case of $YBa_2Cu_3O_{7-y}$ and Bi, Ca and O in the case of Bi - Ca - Sr - Cu - O as can be seen from figure 5.3 (b) and 5.4 (b) respectively. In the case of both thin films the Si substrate is clearly visible. EDX is clearly not as sensitive as RBS in determining the presence of different elements. No EDX was done for film on carbon fiber substrate since any free cabon fibres in the electron microscope may interfere with the lenses.

5.2.3 SQUID Measurement

Measurements were made on a number of sample of Y-based and

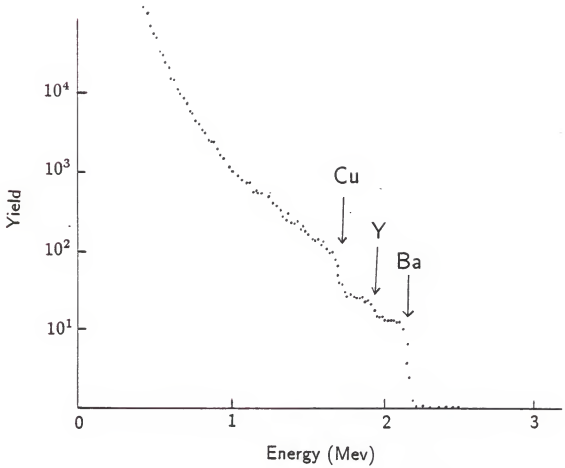

Fig. 5.1 (a) RBS plot for $YBa_2Cu_3O_{7-y}$ bulk material.

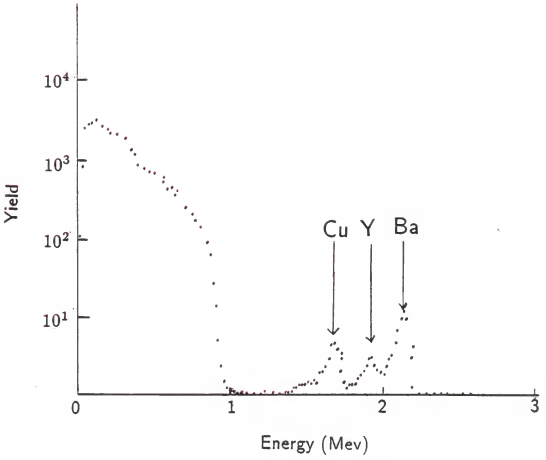

Fig. 5.1 (b) RBS plot for $YBa_2Cu_3O_{7-y}$ thin film of thickness 500 Å.

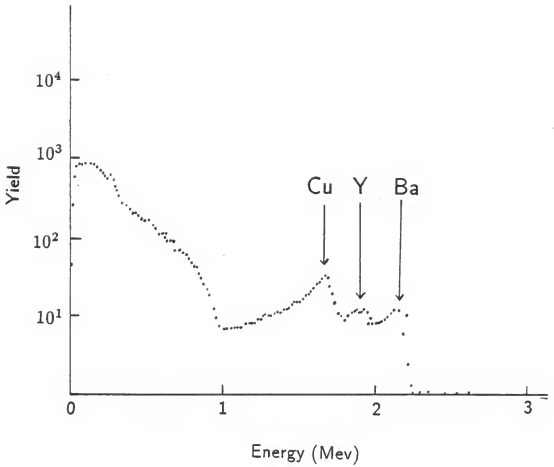

Fig. 5.1 (c) RBS plot for $YBa_2Cu_3O_{7-y}$ thin film of thickness 1000 Å.

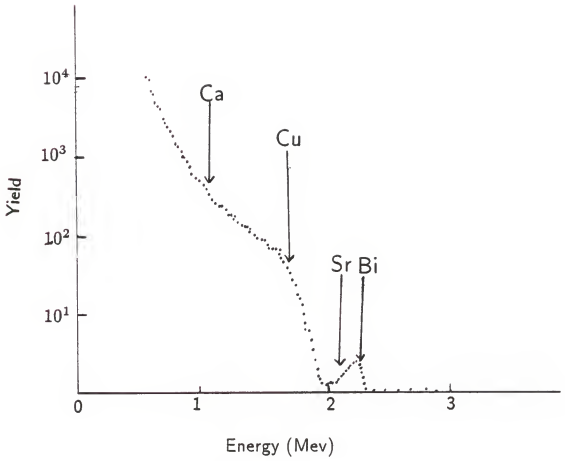

Fig. 5.2 RBS plot for $Bi_2Ca_1Sr_2Cu_2O_{8-y}$ thin film.

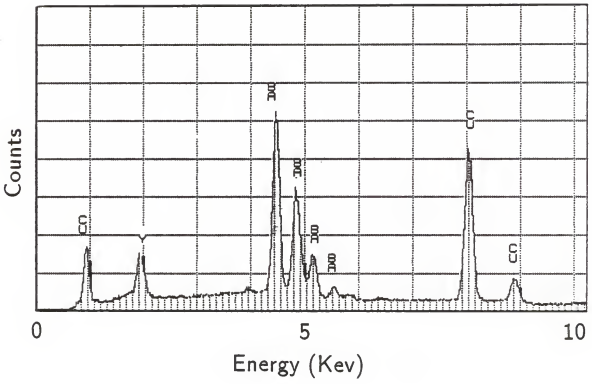

Fig. 5.3 (a) EDXA plot for $YBa_2Cu_3O_{7-y}$ bulk material.

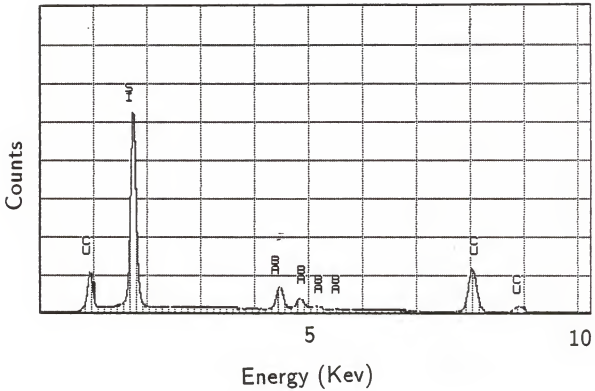

Fig. 5.3 (b) EDXA plot for $YBa_2Cu_3O_{7-y}$ thin film.

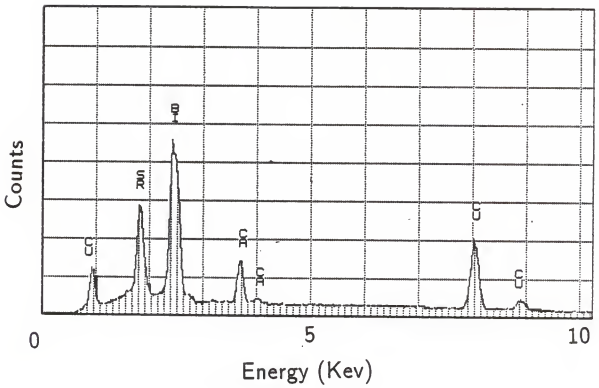

Fig. 5.4 (a) EDXA plot for $Bi_2Ca_1Sr_2Cu_2O_{8-y}$ bulk material.

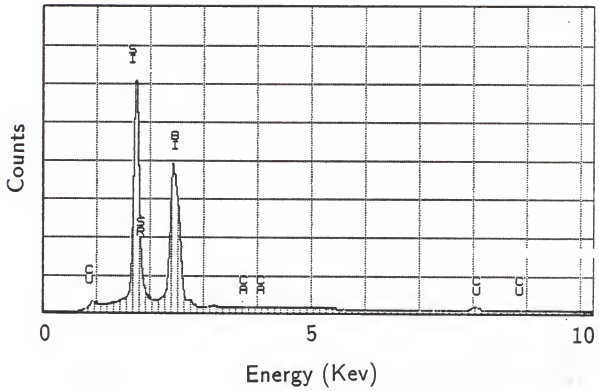

Fig. 5.4 (b) EDXA plot for $Bi_2Ca_1Sr_2Cu_2O_{8-y}$ thin film.

Bi-based superconductors. A 0.1 cm^2 would have volume susceptibility

$$\chi = (-1/4\pi)V \approx 10^{-7}/4\pi$$

yields a moment of $\approx 10^{-5}$ emu/g at 1000 Oe compared to a susceptibility for Si 10^{-6} emu/g which yields a moment of $\approx 10^{-5}$ emu/g.

The background in the SQUID after cycling the field to 55 kOe and back to zero was large (-1.2X10^{-4} emu), and decreased with time by a factor of 10 after about 10 minutes. This background was not a function of temperature and its source is probably persistent currents in the pick-up coils induced by cycling the applied field.

Signals from bulk materials were in the 10^{-2} emu range (actual values in this work are given in emu/g) and so the background was not important. The thin film signal was smaller than the background and so a correction was required. It was found that after annealing the Y - Ba - Cu - O thin film at 700° C for 4 hours a small diamagnetic response was obtained at 10 K after subtraction of the background indicating thatt the film was superconducting.

5.2.4 Resistivity

The thin films on Si were not strongly adhesive and could be damaged so that making contacts by pressure to measure resistivity is not advisable. We therefore used a silver Epoxy to attach wires to the sample. This epoxy reacted with the film and discolored the superconductor and no superconducting transition was detected in resistivity. We are now coating the ends of the sample with evaporated Al and applying the epoxy on the Al in the hope that the Al will act as a buffer layer against reactions between the epoxy and superconductor.

5.3 Carbon Fiber substrate

Carbon fibers are supplied by Peter Sherwood in chemistry. They are less than a $1\mu m$ thick. Samples are arranged in bundles of 1000 - 5000 fibers and the superconductor was deposited on one side by laser ablation. The deposited film was grey in color. It was found that the C-fibers oxidize rapidly at $350°C$ while at $300°C$, the sample could be annealed for an hour with no visible effects on the C-fiber.

5.3.1 X-ray Photoeletron Spectroscopy (XPS)

XPS measurments were made using a VSW HA 100 spectrometer with a base pressure of 10^{-10} TORR using Mg K X-radiation by Prof. Sherwoods group. we will report only the results here. XPS study showed the presence of all the 5 elements,Bi, Sr, Ca, Cu and O in thin film of $Bi_2SrCa_2Cu_2O_{8-x}$ deposited on carbon fiber.

5.3.2 SQUID Measurement

In the case of C- fiber films no clear results were obtained since the signal was approximately the same size as the background after annealing at 300° C.

5.3.3 Resistivity

We are using silver epoxy to attach wires to the sample. But the epoxy reacted with superconductor so now we are coating end of the sample with evaporated Al and applying the epoxy on the Al. We find that the carbon fiber resistance does not change with the temperature. We did not see any change in the resistance of the film on the carbon fiber. Therefore, the film is not a superconductor.

CHAPTER 6

CONCLUSION

We have prepared Y- based and Bi- based superconductors. It is observed that in the Y- based sample replacement of Y by another rare earth element decreases the transition temperature slightly. Replacement of Cu by a small percentage of Co decreases the transition temperature drastically. This confirms that metallic Cu is necessary for high a transition temperature and the rare earth is not very important for superconductivity.

We were sucessful in making thin films of superconductors on Si by laser ablation. It was observed that a vaccum was required to prepare the thin film. We hope to get better results with our new improved vacuum chamber in the future, but our peliminary study is quite encouraging. From the RBS, XPS, and EDX results we can see that all the elements of bulk superconductors are present in thin film. It is also found that post-preparation annealing of the thin film is required for the film to exhibit superconductivity.

In the case of the carbon fiber substrate we observed that C-fibers oxidize rapidly at 350° C but for the thin film to be a superconductor post annealing at temperatures 600° C or higher are required. No superconductivity was found on as deposited C-fibers or c-fibers annealed at 300° C.

REFERENCES

1. H. Kamerlingh Onnes, Leiden Comm. 120 b, 124 c (1911).
2. J.G. Bednortz and K.A. Muller, Z. Phys. B 64, 189 (1986).
3. M.K. Wu, J.B. Ashburn, C.J. Torng, P.H. Hor, R.L. Meng, L. Gao, Z.J. Huang, Y.Q. Wang and C.W. Chu, Phys. Rev. Lett. B 8, 908 (1987).
4. H. Maeda, Y. Tanaka, M. Fukutomi and T. Asano, Japan Jour. Appl. Phys. lett. 27, L209 (1988).
5. C.W. Chu, J. Bechtold, L. Gao, P.H. Hor, Z.J. Huang, R.L. Meng, Y.Q. Wang, and Y.Y. Xue, Phys. Rev. Lett. 60, 941 (1988).
6. Z.Z.sheng and A.M. Hermann, Nature 332, 55 (1988).
7. A.M. Hermann and Z.Z. Sheng, D.C. Vier, S. Schultz and S.B. Oseroff, Phys. Rev. B 37, 9742 (1988).
8. M. Kawaski, M. Funabashi, S. Nagata, K. Fueki and H. Koinuma, Jpn. J. Appl. Phys. 26, L388 (1987).
9. R.B. Laibowitz, R.H. Koch, P. Chaudhari and R.J. Gambino Phys. Rev. B 35, 8821 (1987).
10. R. hammond, M. Natio, B. Oh, M. Hahn, P. Rosenthal, A. Marshall, N. Missert, M.R. Beasley, A. Kapitulnic and T.H. Gaballe, MRS Spring Meeting, Anaheim, CA, april (1987).
11. K. Moorjani, J. Bohandy, F.J. Adrian, B.F. Kim, R.D. Shull, C.K. Chiag, L.J. Swartzendurber and L.H. Bennett, Phys. Rev. B 36, 4036 (1987).
12. D. Dijkkamp, T. Venkatesan, X.D. Wu, S.A. Shaheen, N. Jisrawi, Y.H. Min-Lee, W.L. Mclean and M. Croft, Appl. Phys. Lett. 51, 619 (1987)
13. W.A. Sietz and W.W. Webb, Phys.Rev. 178, 657 (1969).

14. M. Hong, S.H. Liou, J. Kwo and B.A. Davidson Appl. Phys. Lett., 51, 694 (1987).

15. C. Webb, S.L. Weng, J.N. Eckstein, N. Missert, K. Char, D.G. Schlom, E.S. Hellman, M.R. Beasley, A. Kapitulnik and J.S. Harris, Appl. Phys. Lett. 51, 1191 (1987).

16. M. Gurvitch and A.T. Fiory, Appl. Phys. Lett. 51, 1027 (1987).

17. A. Mogro-Campero, B.D. Hunt, L.G. Turner, M.C. Burrell and W.E. Blaz Appl. Phys. Lett. 52, 584 (1988).

PREPARATION AND CHARACTERIZATION OF Y- AND Bi-BASED BULK AND THIN FILMS SUPERCONDUCTORS

by

NITYANAND SINGH

M.SC., I.I.T.,Kharagpur,India,1986

AN ABSTRACT OF A MASTER'S THESIS

submitted in partial fulfillment of the
requirements for the degree

MASTER OF SCIENCE

Department of Physics

Kansas State University

Manhattan, Kansas

1989

ABSTRACT

We have prepared Y- based and Bi- based bulk superconductors by solid state reaction and thin films of superconductor on Silicon and Carbon fiber substrates by laser ablation using a pulse excimer laser. The structure of the bulk material was studied using X-rays. The chemical composition and profile of the bulk material and thin films were studied using X-ray photoelectron spectroscopy (XPS) and Rutherford backscattering spectroscopy (RBS). Magnetic properties of superconductors were studied using a SQUID magnetometer and an AC susceptibility probe down to liquid He temperature. Resistivity measurement were performed using the four probe method down to liquid He temperature. All the bulk materials showed superconductivity with the transition temperature depending on the amount of Co substituted for Cu. The thin films on silicon substrates showed superconductivity at low temperatures but those on carbon fibers did not show any indication of superconductivity.